Appl Phys B (2009) 95: 691–695
DOI 10.1007/s00340-009-3471-6

Applied Physics B
Lasers and Optics

Diode-pumped passively mode-locked Nd:CTGG disordered crystal laser

G.Q. Xie · D.Y. Tang · W.D. Tan · H. Luo · S.Y. Guo · H.H. Yu · H.J. Zhang

Received: 30 October 2008 / Revised version: 23 February 2009 / Published online: 2 April 2009

Abstract A diode-pumped passively mode-locked Nd:CTGG disordered crystal laser has been experimentally demonstrated for the first time to our knowledge. Mode locked with a semiconductor saturable absorber mirror, the laser generated 5.2 ps pulses at a repetition rate of 88 MHz. After intracavity dispersion compensation, the mode-locked pulses were shortened to 4.3 ps. Multiple emission wavelengths of the Nd:CTGG laser could be synchronously mode locked under dispersion compensation.

PACS 42.70.Hj · 42.60.Fc · 42.55.Xi

1 Introduction

Neodymium-doped (Nd-doped) disordered crystals have attracted much attention as a new type of laser materials at 1.06 μm [1, 2]. Owing to the random distribution of cationic ions in some lattice sites, multiple structural centers exist in the disordered crystal. The presence of multiple structural centers causes the considerable inhomogeneous broadening and splitting of the spectral lines in the disordered crystals. The broad absorption and fluorescence spectra of the disordered crystals favor efficient diode pumping and ultrashort mode-locked pulse generation. In addition, the disordered crystals have better thermal property than Nd:glass, which is in favor of high average power output.

So far, Nd-doped calcium niobium gallium garnet (Nd:CNGG) and calcium lithium niobium gallium garnet (Nd:CLNGG) disordered crystals have been developed [3, 4]. The Nd:CNGG and Nd:CLNGG have a common garnet structure and the Nb^{5+}, Ga^{3+} distribute randomly in crystal lattices sites, resulting in broadening and splitting of the spectral lines. Optically transparent Nd:CNGG disordered crystal is a nonstoichiometric compound, and cationic vacancies exist in the Nd:CNGG crystal lattices. By introducing Li^{+} to fill in the cationic vacancies, Nd:CLNGG disordered crystal is synthesized. Nd:CLNGG disordered crystal has a more stable stoichiometric structure. CW and mode-locking operations of the Nd:CNGG and Nd:CLNGG disordered crystal lasers have been reported [5–10]. The Nd-doped calcium tantalum gallium garnet (Nd:CTGG) has a similar garnet structure as Nd:CNGG. Recently, Guo et al. have reported the growth and characterizations of the Nd:CTGG disordered crystal [11]. However, no mode-locking operation of Nd:CTGG laser has been reported to date.

In this paper we report on a diode-pumped passively mode-locked Nd:CTGG disordered crystal laser for the first time. The mode locking of the laser was started and sustained by a semiconductor saturable absorber mirror (SESAM). Without dispersion compensation, the Nd:CTGG mode-locked laser generated stable 5.2 ps mode-locked pulses at a repetition rate of 88 MHz, and the mode-locked spectral band of the Nd:CTGG laser was accompanied by multiple CW spectral lines. After intracavity dispersion compensation made with a pair of prisms, the mode-locked pulses were shortened to 4.3 ps. In this case extra spectral lines of the Nd:CTGG laser could also become mode-locked and multiple-wavelength synchronous mode locking

G.Q. Xie (✉) · D.Y. Tang · W.D. Tan · H. Luo
School of Electrical and Electronic Engineering, Nanyang Technological University, Singapore 639798, Singapore
e-mail: gqxie@ntu.edu.sg
Fax: +65-679-04161

S.Y. Guo · H.H. Yu · H.J. Zhang
State Key Laboratory of Crystal Materials and Institute of Crystal Materials, Shandong University, Jinan 250100, China

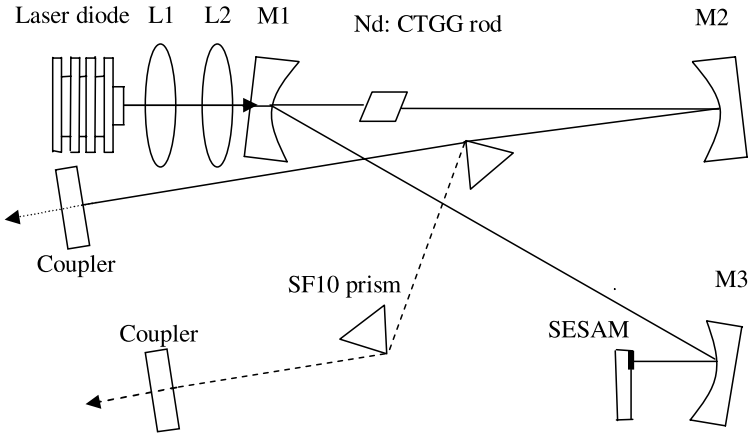

Fig. 1 Experimental setup of the mode-locked Nd:CTGG laser. ROCs (radius of curvature) of M1, M2, M3 are 10, 30, 10 cm, respectively

was achieved. In this paper we mainly focus on the mode-locking performance of the Nd:CTGG disordered crystal laser. The detailed spectroscopic and structural properties of Nd:CTGG will be further investigated.

2 Experimental setup

The mode-locked laser setup is schematically shown in Fig. 1. A single-emitter laser diode was used as the pump source. The emission wavelength of the laser diode varied in the range of 802–807 nm with the output power strength. It is noted that the wavelength shift of the laser diode may change the proportion that the various structural centers are excited, thus alters the spectral composition of the laser spectrum. The pump light was focused into the Nd:CTGG crystal by two coupling lenses with the same focal length of 8 cm. The focused pump spot size in the crystal was 100 μm × 250 μm. The Nd:CTGG disordered crystal was grown by the Czochralski method. The concentration of Nd^{3+} was 2 at.% in the melt. The Nd:CTGG rod used in our experiments had dimensions of 3×3 mm^2 in cross section and 3 mm in length. In order to remove the generated heat in the crystal for effective laser operation, the Nd:CTGG rod was wrapped in indium foil and mounted tightly in a water-cooled copper holder that was maintained at a temperature of 15°C. Both sides of the crystal were antireflection coated at the pump and laser wavelengths. Under mode-locking operation, the crystal was placed with small incidence angle with respect to the cavity axis to suppress the Fabry–Perot etalon effect. A standard X-folded cavity was used in the experiment to achieve a suitable focusing spot on the SESAM and simultaneously an optimum mode matching with pump in the laser crystal. The laser mode sizes in the crystal and on the SESAM were calculated to be ∼45 and ∼35 μm in radius, respectively. A SESAM with a saturable absorption of 1% was used to start and sustain the mode locking of the laser. A pair of SF10 prisms with a tip–tip distance of 49 cm was used to compensate the cavity dispersion. The cavity length was kept the same when the prisms were inserted. The transmission of the two output couplers was 1.5%.

3 Results and discussion

When the SESAM was replaced with a high-reflective plane mirror, and no prisms was within the cavity, the laser operated in a CW mode. Figure 2 shows the relationship of the CW output power versus the absorbed pump power. The output coupler used in the experiment had a transmission of 1.5%. Despite of the transmission losses caused by multiple cavity mirrors, the laser threshold was as low as 0.21 W of the absorbed pump power. A maximum CW output power of 0.63 W was obtained under an absorbed pump power of 3.75 W. The corresponding laser slope efficiency was 20%. Using the SESAM as an end mirror (Fig. 1), stable mode locking could be achieved. Without inserting the prisms in the cavity, the maximum average output power was 107 mW, achieved under 3.57 W of the absorbed pump power with slope efficiency of 3.6% (Fig. 2). The low slope efficiency could be attributed to the large nonsaturable loss of the SESAM and the reflection loss of the crystal mounted with a tilting angle.

Stable CW mode locking could be achieved in the laser only when the absorbed pump power was beyond 2.3 W, below which the laser showed unstable Q-switched mode locking. With a high-speed detector and 1 GHz bandwidth oscilloscope, we measured the mode-locked pulse trains. Figures 3a and 3b show the CW mode-locked pulse trains in the ns and μs timescales, respectively. The mode-locked pulses have a repetition rate of 88 MHz corresponding to the laser cavity length of 1.7 m. The pulse to pulse intensity fluctuation is estimated to be less than 3%. In the experiment, the CW mode locking state could be sustained for several hours.

The autocorrelation trace of the mode-locked pulses was measured with a commercial noncollinear autocorrelator. It is shown in Fig. 4a. The autocorrelation trace is well fit-

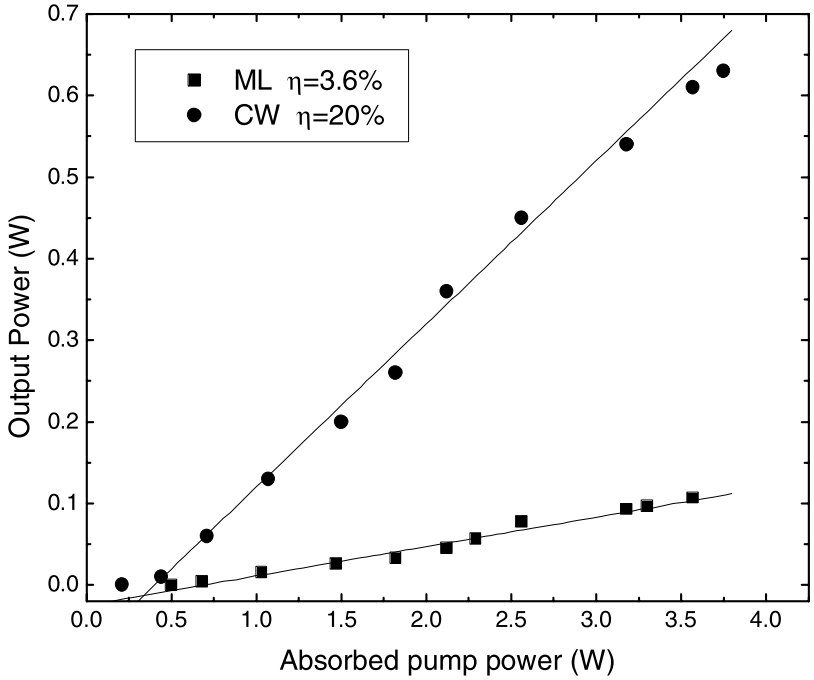

Fig. 2 Relationship of the output power versus absorbed pump power under CW and mode-locking operations

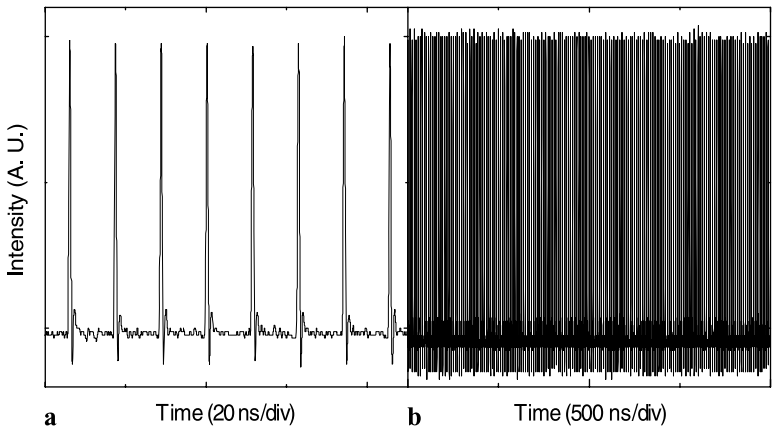

Fig. 3 CW mode-locked pulse trains in ns (**a**) and μs (**b**) timescales

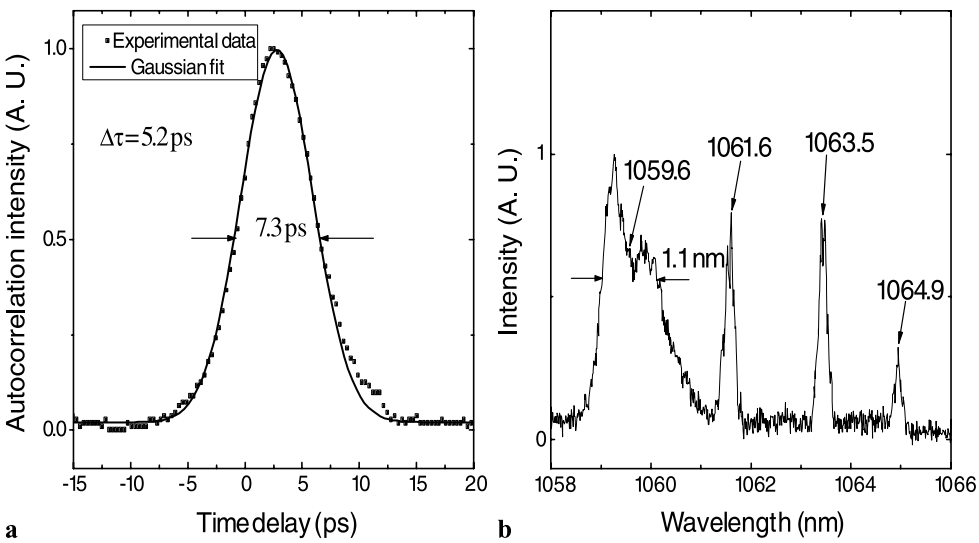

Fig. 4 The measured autocorrelation trace (**a**) and optical spectrum (**b**) of the mode-locked pulses in the case without dispersion compensation

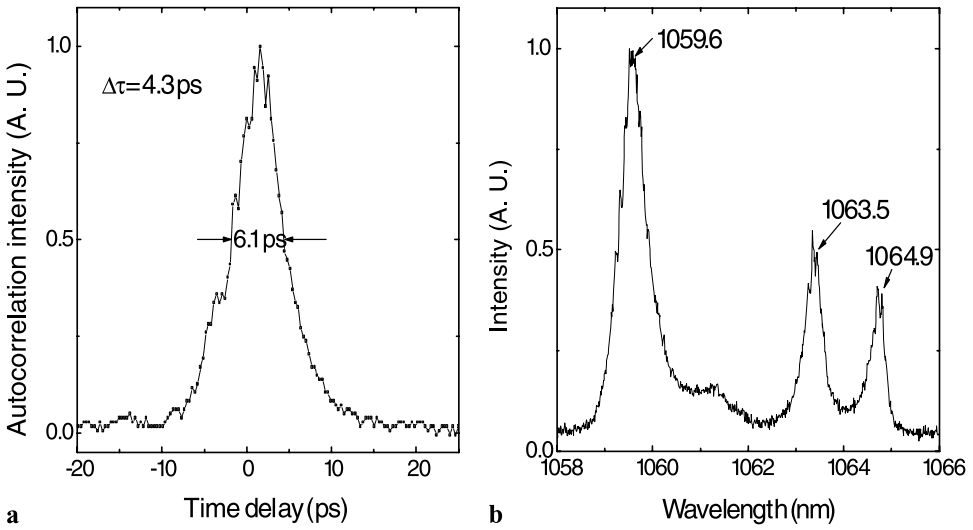

Fig. 5 The measured autocorrelation trace (**a**) and optical spectrum (**b**) of the synchronously mode-locked pulses under dispersion compensation

ted with Gaussian profile. The autocorrelation trace has a FWHM of 7.3 ps. Assuming a Gaussian pulse shape, the mode-locked pulse duration was 5.2 ps. The mode-locked pulse spectrum was measured by an optical spectrum analyzer with a resolution of 0.05 nm. It is shown in Fig. 4b. Besides the mode-locked band centered at 1059.6 nm, there also exist three narrow CW spectral lines at 1061.6, 1063.5, and 1064.9 nm respectively. The CW emissions at these wavelengths are caused by the special Nd:CTGG gain spectrum. We think the extra gain spectral lines are generated by different Nd^{3+} structural centers in Nd:CTGG disordered crystal. Under strong pumping these gain lines can also reach the lasing threshold. The narrow CW spectral bandwidths are a result of narrow gain line widths of Nd:CTGG at these wavelengths. We note that a CW component also exists in the mode-locking band centered at 1059.6 nm. The actual mode-locked spectral bandwidth should be less than 1.1 nm.

Mode-locking performance of the laser after cavity dispersion compensation was further experimentally investigated. We used a pair of SF10 prisms in the cavity for the dispersion compensation (Fig. 1). After inserting the prisms, the average output power of the laser had no obvious change, and CW mode locking could still be achieved. The mode-locked pulse trains had the same repetition rate of 88 MHz. By autocorrelation scanning, we further verified that there was only one mode-locked pulse circulating in the cavity. Figures 5a and 5b show the autocorrelation trace and optical spectrum of the mode-locked pulses obtained. Comparing Fig. 4b and Fig. 5b it is seen that after dispersion compensation, the CW emission at 1061.6 nm was suppressed. Moreover, the three gain spectral bands centered at the wavelengths of 1059.6, 1063.5, and 1064.9 nm became simultaneously mode locked. As there was only one circulating pulse in the cavity, it suggested that the three gain bands were synchronously mode locked. The synchronous mode locking of the three gain bands under cavity dispersion compensation could be understood as the following: without dispersion compensation, light generated by each of the spectral bands has different propagation speed in the cavity. As the light generated by the weak spectral bands could not saturate the SESAM by itself, no mode locking could be achieved on them. After dispersion compensation, light generated by all the spectral bands has the same group velocity. Therefore, saturation of the SESAM caused by light of one spectral band would also have the same effect on the light of other bands which leads to the mode locking of the other bands. Because their mode locking is caused by the cross saturation of the absorber, their mode locking is so synchronized that the generated mode-locked pulses are temporally overlapped in the cavity. We note that the suppression of the spectral peak at 1061.6 nm implies the existence of homogenous broadening in the Nd:CTGG gain profile. The strong emission at 1059.6 nm exhausted the gain at 1061.6 nm. The widest mode-locking band was at 1059.6 nm with bandwidth of 0.6 nm. The synchronously mode-locked pulses have a pulse duration of 4.3 ps (Fig. 5a). In addition, slight modulation is observable in the autocorrelation trace, which may be a result of optical beating between the pulses mode locked by different spectral bands [7].

It is worth comparing the mode-locking performance of the different disordered crystals, Nd:CNGG, Nd:CLNGG, Nd:CTGG, and the ordered crystal Nd:GGG (Table 1). The Nd:GGG ordered crystal has very narrow gain line width. Thus the mode-locked pulses of the laser have long duration [12]. Owing to the inhomogeneous broadening caused by the disordered crystal structures, the Nd^{3+}-doped disordered crystals have broader gain line widths, therefore, these disorder crystals lasers can emit shorter mode-locked pulses. Among these disordered crystals, the Nd:CNGG has dual-gain spectral lines with comparable line widths

Table 1 The mode-locking results comparison of Nd:CNGG, Nd:CLNGG, Nd:CTGG disordered crystals lasers and Nd:GGG ordered crystal laser

	Nd:CNGG [7]	Nd:CLNGG [10]	Nd:CTGG	Nd:GGG [12]
Pulse duration	5 ps	2 ps	4.3 ps	17.5 ps
Pulse spectrum	2 spectral lines (0.5 nm width each)	1 spectral line (1.2 nm width)	3 spectral lines (max. 0.6 nm width)	1 spectral line (0.26 nm width)
Average output power	90 mW	101 mW	∼107 mW	400 mW
Slope efficiency	3.5%	8.9%	3.6%	–

(∼0.5 nm), its mode-locked pulses have a duration of 5 ps. The Nd:CLNGG has a single gain line of ∼1.2 nm line width. Its mode-locked pulses have much shorter pulse duration (2 ps). The Nd:CTGG has several gain lines but only three of them could be simultaneously mode locked. Among the three mode-locked gain lines, the broadest one has a bandwidth of 0.6 nm. The synchronously mode-locked pulses of the laser have durations of 4.3 ps. To sum up, the Nd:CLNGG is advantageous for the generation of shorter mode-locked pulses, however, Nd:CNGG and Nd:CTGG can be used for dual- or multiwavelength mode-locked lasers. The three disordered crystal lasers have comparable average output power under similar pump conditions, but the Nd:CLNGG laser has the highest slope efficiency.

As reported before in the Nd:CNGG and Nd:CLNGG [13, 14], at least five nonequivalent Nd^{3+} centers exist in these disordered crystals. The various Nd^{3+} centers have their own unique fluorescence spectra which results in the inhomogeneous broadening and splitting of spectral lines in the disordered crystals. The Nd:CTGG has a similar disordered structure to Nd:CNGG, thus the inhomogeneous broadening and splitting of spectral lines should also exist in the Nd:CTGG. At present, the specific energy level structure of Nd:CTGG has not been studied yet. Dual-wavelength emission has been reported for the Nd:CNGG mode-locked laser [7]. Compared with the Nd:CNGG laser, Nd:CTGG disordered crystal laser has more emission spectral lines which implies that the Nd:CTGG should have a different energy level structure. The dual- and multiple-wavelength emissions of disordered crystals could be useful for optical beat generation, THz-wave coherent radiation, etc. [15, 16].

4 Conclusion

In conclusion, we have experimentally demonstrated a diode-pumped passively mode-locked Nd:CTGG disordered crystal laser. With a SESAM as a mode locker, stable CW mode locking has been achieved. Without dispersion compensation, the laser generated mode-locked pulses with pulse durations of 5.2 ps, repetition rate of 88 MHz, and average output power of 107 mW. After dispersion compensation by using a pair of prisms in the cavity, three-wavelength synchronously mode-locked pulses have been generated with pulse durations of 4.3 ps. Our experimental results have shown that the Nd:CTGG could be potentially useful for multiple-wavelength lasers.

Acknowledgement The work is partially supported by the National Research Foundation Singapore under the contract NRF-G-CRP 2007-01.

References

1. M.H. Ober, E. Sorokin, I. Sorokina, F. Krausz, E. Wintner, I.A. Shcherbakov, Opt. Lett. **17**, 1364 (1992)
2. H.J. Eichler, D. Ashkenasi, H. Jian, A.A. Kaminskii, Phys. Status Solidi A Appl. Res. **146**, 833 (1994)
3. K. Shimamura, M. Timoshechkin, T. Sasaki, K. Hoshikawa, T. Fukuda, J. Cryst. Growth **128**, 1021 (1993)
4. L. Gheorghe, M. Petrache, V. Lupei, J. Cryst. Growth **220**, 121 (2000)
5. P.K. Mukhopadhyay, K. Ranganathan, J. George, S.K. Sharma, T.P.S. Nathan, Opt. Laser Technol. **35**, 173 (2003)
6. K. Naito, A. Yokotani, T. Sasaki, T. Okuyama, M. Yamanaka, M. Nakatsuka, S. Nakai, T. Fukuda, M.I. Timoshechkin, Appl. Optics **32**, 7387 (1993)
7. G.Q. Xie, D.Y. Tang, H. Luo, H.J. Zhang, H.H. Yu, J.Y. Wang, X.T. Tao, M.H. Jiang, L.J. Qian, Opt. Lett. **33**, 1872 (2008)
8. T.T. Basiev, N.A. Eskov, A.Y. Karasik, V.V. Osiko, A.A. Sobol, S.N. Ushakov, M. Helbig, Opt. Lett. **17**, 201 (1992)
9. A. Agnesi, S. Dell'Acqua, A. Guandalini, G. Reali, F. Cornacchia, A. Toncelli, M. Tonelli, K. Shimamura, T. Fukuda, IEEE J. Quantum Electron. **37**, 304 (2001)
10. H. Luo, D.Y. Tang, G.Q. Xie, W.D. Tan, H.J. Zhang, H.H. Yu, Opt. Commun. **282**, 291 (2009)
11. S.Y. Guo, D.R. Yuan, C.X. F, H.H. Yu, S.Q. Sun, F.P. Yu, H.J. Zhang, H.R. Xia, X.T. Tao, J. Cryst. Growth **311**, 214 (2008)
12. L.J. Qin, D.Y. Tang, G.Q. Xie, H. Luo, C.M. Dong, Z.T. Jia, H.H. Yu, X.T. Tao, Opt. Commun. **281**, 4762 (2008)
13. A. Lupei, V. Lupei, L. Gheorghe, L. Rogobete, E. Osiac, A. Petraru, Opt. Mater. **16**, 403 (2001)
14. Y.K. Voronko, A.A. Sobol, A.Y. Karasik, N.A. Eskov, P.A. Rabochkina, S.N. Ushakov, Opt. Mater. **20**, 197 (2002)
15. M.D. Pelusi, H.F. Liu, D. Novak, Y. Ogawa, Appl. Phys. Lett. **71**, 449 (1997)
16. K. Miyamoto, H. Minamide, M. Fujiwara, H. Hashimoto, H. Ito, Opt. Lett. **33**, 252 (2008)